Electronic Supplementary Material for CrystEngComm

Crystal structures with a challenge: high-pressure crystallisation of ciprofloxacin sodium salts and their recovery to ambient pressure

Francesca P. A. Fabbiani, Birger Dittrich, Alastair J. Florence, Thomas Gelbrich, Michael B. Hursthouse, Werner F. Kuhs, Norman Shankland and Heidrun Sowa

Electronic Supplementary Information

Contents:

Further structure solution and refinement details for structure 1

The structure was solved using data to 46.8° 2θ, comprising 207 reflections. The SA structure solution involved the optimisation of one molecule of ciprofloxacin, totalling 9 degrees of freedom (3 positional, 3 orientational and 3 torsional). All degrees of freedom were assigned random values at the start of the simulated annealing. The best SA solution had a favourable χ^2SA \ χ^2Pawley ratio of *ca.* 10, a chemically reasonable packing arrangement and exhibited no significant misfit to the data. The solved structure was subsequently refined against data in the range 5.0 - 69.04° 2θ (1.369 Å resolution, 617 reflections). The restraints were set such that bonds and angles did not deviate more than 0.01 Å and 1° respectively, from their initial values during the refinement. Atoms C(1), N(1), C(5), H(51), C(6), C(7), C(8), O(3), C(9), C(1)0, H(101), C(11), F(1), C(12), C(17), H(171), C(4) and N(2) were restrained to be planar. A spherical harmonics (4th order) correction of intensities for preferred orientation was applied in the final refinement.[1]

Further structure refinement details for structures 3-6

Owing to the lower data quality and resolution, and lower data to parameter ratio, vibration and thermal similarity restraints were used for **3**. The refinement of **5** proved to be the most challenging, owing to the low scattering power of the recovered crystal and broad and at times split reflection profiles. Though broad and split reflection profiles were also observed in **3** and to some extent in **6**, they were much more pronounced in **5**. For the structure of **5**, the TLS formalism was used to constrain ADPs of the quinoline fragment of the Cf moiety. The use of this formalism for curing of ill-defined ADPs is well known. One least-squares parameter was assigned for the ADPs of the atoms in the carboxylate fragment, one for those in the piperazine fragment and one for those in the cyclopropyl fragment of each independent molecule in the asymmetric unit. ADPs for carbonyl oxygen, fluorine and sodium atoms were freely refined. Water O-atoms were refined with a mixture of isotropic and anisotropic thermal parameters. The U_{iso} for axial O(100) in **4** is larger than expected and strongly suggests disorder; we were however unable to build a suitable model. In the structure of **5**, O(1031)-O(1031) and O(1050) – O(1051) form two pairs of 40%-60% and 50%-50% disordered atoms, respectively. O(106) is 50% occupied, and we were unable to model its disordered counterpart satisfactorily and we assign this problem to the poor data quality. This would give 9.5 water molecules in the asymmetric unit, or 4.75 water molecules per Cf moiety. Given that the structures of **4** and **6** each contain five water molecules, it can be assumed that this should be the same for the structure of **5**.

Additional figures to structures 2-6

Figures 1 and 2 depict the bonding environment of structures **2**, **3**, **4** and **6**.

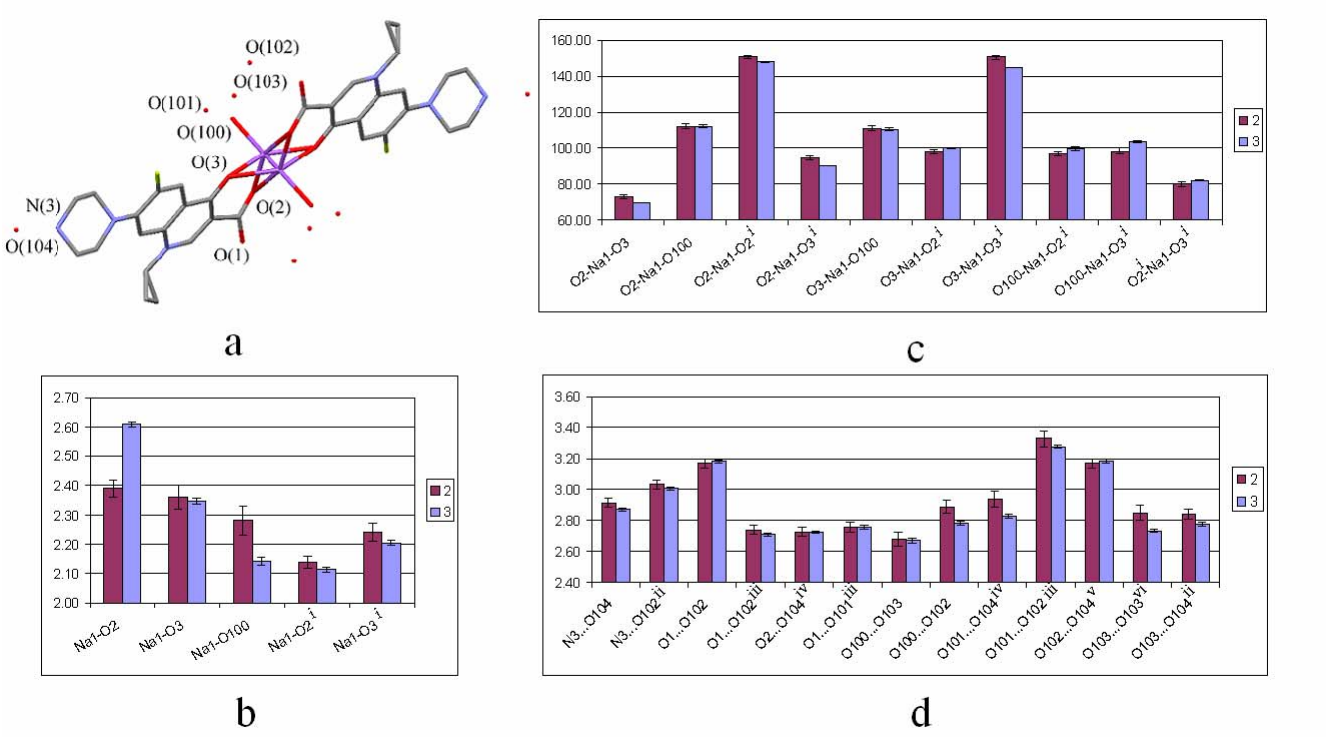

Fig. 1 a) Ciprofloxacin: Na-cation dimer in the crystal structures of **2** and **3**. H-atoms and disordered O-atoms have been omitted for clarity. The numbering scheme is given for the atoms in the asymmetric unit involved in H-bonding; b) variation in Na-O bonded distances in **2** and **3**; c) variation in O-Na-O angles in **2** and **3**; d) variation in H-bonding donor…acceptor distances in **2** and **3**. Only the major, 80 %, disordered part for O100 in the structure of **3** was considered. All e.s.d.s were calculated with PLATON[2] for consistency. Symmetry codes: i) -x,1-y,2-z; ii) -x,-y,1-z; iii) 1-x,1-y,2-z; iv) -x,1-y,1-z; v) 1+x,y,1+z; vi) -x,-y,2-z

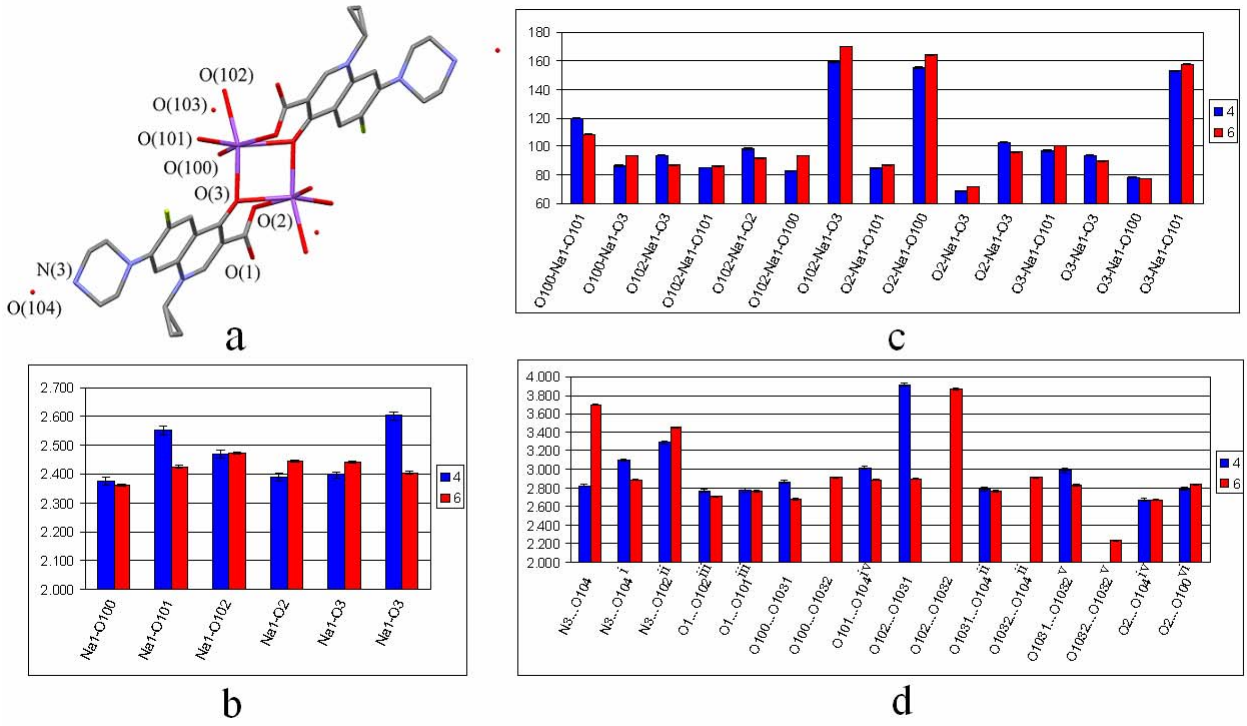

Fig. 2 a) Ciprofloxacin: Na-cation dimer in the crystal structures of **4** and **6**. H-atoms and disordered O-atoms have been omitted for clarity. The numbering scheme is given for the atoms in the asymmetric unit involved in H-bonding; b) variation in Na-O bonded distances in **4** and **6**; c) variation in O-Na-O angles in **4** and **6**; d) variation in hydrogen-bonding donor…acceptor distances in **4** and **6**. O1031 and O1032 refer to 50 % disordered atoms in **6**, for **4** O103 was used for comparison. All e.s.d.s were calculated with PLATON[2] for consistency. Symmetry codes: i) 1-x,-y,-z; ii) –x,-y,1-z; iii) 1-x,1-y,2-z; iv) –x,1-y,1-z; v) –x,-y,2-z; vi) –x,1-y,2-z

Rationale behind the unit cell choice for structure 5

Indexing of the reflections obtained from the 100 K data collection of **5**, gave a unit cell with dimensions substantially different from **4** and with approximately double the volume. A closer inspection revealed that the two unit cells are in fact closely related: the unit cell of **5** can be transformed to a unit cell that is similar to that of **4**, even more so to that of **2**, by the matrix:

$$\begin{pmatrix} 0 & -1/2 & -1/2 \\ 0 & -1/2 & 1/2 \\ -1 & 0 & 0 \end{pmatrix}$$

The resulting unit-cell parameters are: a = 9.479(6) Å, b = 9.643(6) Å, c = 11.065(10) Å, α = 85.756(15) °, β = 98.759(14) °, γ = 93.07(7) °, V = 996.0(12) Å^3. We do not believe that the differences between this unit cell and those of **2** and **4** are particularly significant, other than in testifying to a change in the coordination environment of the Na-cations and Cf moieties. The larger supercell, with which all reflections could be indexed, was chosen for data integration. Intensity statistics $I/\sigma(I)$ for the $k + l$ even and odd reflections are 2.86 and 1.89, respectively. $k + l$ odd reflections are the weak supercell reflections (see Fig. 3 for reciprocal lattice plots).

The quality of the data is low, but sufficient to identify the main structural features. The data quality and refined structural parameters could also indicate that the structure is in fact modulated. The small cell given above could in principle be used to describe a commensurately modulated structure in (3 + 1)-dimensional superspace with one Cf molecule, five water molecules and two half-occupied Na-cations in the asymmetric unit. Within this model, diffracted intensities are interpreted as main and satellite reflections and indexed by four integers *hklm*. A similar example has been described for the α-form of p-chlorobenzamide.[3] The modulated model was not investigated in our case and will be the subject of a future investigation. Refinement of the unmodulated structure using the smaller cell did not only give rise to a disordered model, but also did not improve the quality of the refinement .The current description of structure **5** is to the best of our knowledge the most suited description for the given data quality.

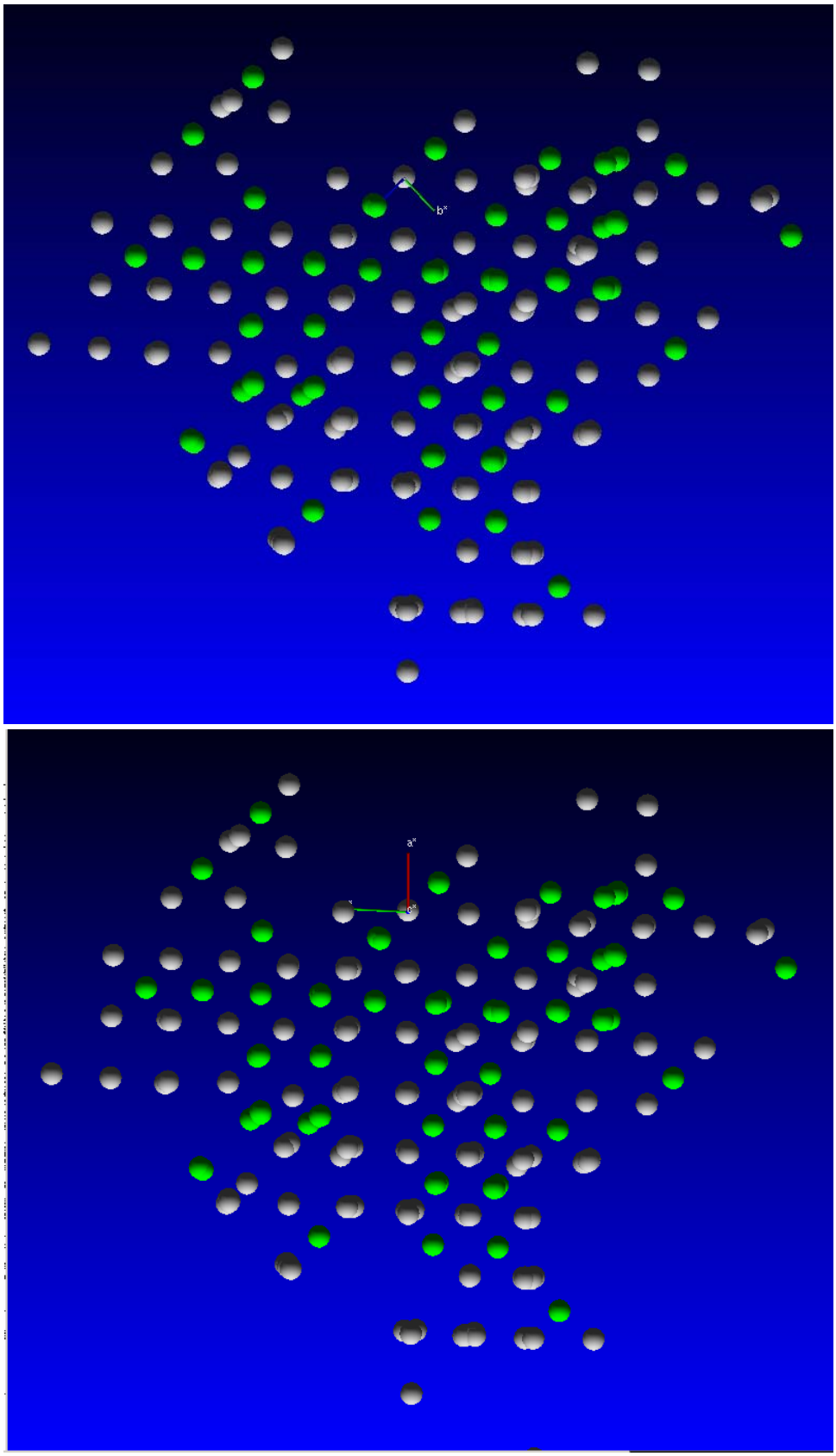

Fig. 3. Reciprocal lattice plots for 5 indexed with (a) the large unit cell (viewed ⊥ to *a**) and (b) the small unit cell. The weak super cell reflections are depicted in green and are not indexed in (b).

Comparison of the structures using H-stripped Hirshfeld surfaces

An effective method for comparison of structures containing molecules in different environments is the use of fingerprint plots derived from Hirshfeld surfaces.[4] Since the Hirshfeld surfaces and the corresponding fingerprint plots are unique for any crystal structure, they provide a powerful tool for elucidating and comparing intermolecular interactions, as well as for spotting common features/trends in specific classes of compounds.[5] The fingerprint plots can be compared qualitatively, as in this work, or quantitatively, via correlation coefficients.[6] The Hirshfeld surface, so named because it derives from Hirshfeld's stockholder partitioning, divides the crystal into regions where the electron distribution of a sum of spherical atoms for the molecule (the promolecule) dominates the corresponding sum over the crystal (the procrystal).[4] According to this definition, all the atoms that comprise the molecule are taken into account, that is H-atoms are also included in the calculation. However, H-atom positions cannot be always determined from X-ray experiments or from geometry considerations alone. This often results in an incomplete structural model, as can for example be the case for H-bonded high-pressure structures. Since Hirshfeld surface partitioning can be regarded as a tool for partitioning space in the crystal, we suggest that certain atom types, H-atoms in this case, can be "stripped" from the molecule and Hirshfeld partitioning subsequently applied. If this procedure is followed for a set of structures, the results obtained from Hirshfeld partitioning are still useful and meaningful, and can give an insight in the different crystalline environments, provided the same approach is used on all structures involved in the comparison. Naturally, these surfaces and derived fingerprint plots should not be compared to those obtained in the usual manner. Hirshfeld surfaces obtained in this way should perhaps also be termed differently to distinguish them from the conventional "Hirshfeld surfaces" pioneered by Spackman et al.. For this purpose, we refer to "H-stripped Hirshfeld surfaces" here.

H-stripped Hirshfeld surfaces and fingerprint plots were obtained for the Cf molecules in the structures **1** – **6** and **8** with Crystal Explorer,[7] and the fingerprint plots are shown in Fig. 4.¶ Since the position of H-atoms involved in H-bonding was not known, all H-atoms coordinates were deleted to produce a self-consistent and comparable set of structures. For the structures **2**-**6**, the H-stripped Hirshfeld surface of each Cf molecule was calculated and the associated fingerprint plot was then filtered so as to show, in colour, the distances between all atoms internal to the surface and all atoms external to it excluding the Na-cations. For structure **5**, which has Z' = 2, two surfaces and two fingerprint pots were calculated. The fingerprint plots in Fig. 4 show that, to a first approximation, Cf molecules in the structures **2**-**6** are in similar environments with respect to neighbouring Cf and water molecules.

This in turn illustrates the qualitative packing similarity of the five structures. The overall shape and colouring of the plots are remarkably similar and this is particularly so within structures that stem from the same high-pressure phase, where the similarity extends to the full fingerprint, i.e. including contacts to Na-cations that appear in the fingerprints as grey shadows. Closer investigation of the regions at large d_e and d_i, which correspond to regions on the Hirshfeld surface without close contacts to neighbouring molecules, confirms these observations and reveals that the degree of similarity of structures **2** and **3** is higher than that of **4** and **6**, as mentioned in earlier paragraphs.

The H-stripped fingerprint plots of the structures of anhydrous Cf (**1**) and Cf hexahydrate (**8**) are also depicted in Fig. 4. Considerations of packing similarity that include **1** and **8** based on fingerprint plots alone is not straightforward, principally because the chemical environments of these two structures, in particular that of **1**, are different from the chemical environments found in **2**-**6**. Consequently, it is perhaps not surprising that to a first approximation the H-stripped fingerprint plots of **1** and **8** show no close similarity to the H-stripped fingerprint plots of **2**-**6**. In particular, we note that the sharp double-tailed feature in 1 corresponds to a head-to-tail interaction

between carboxylate O(2) of one Cf molecule and the terminal N-atom of a piperazine ring of another adjacent Cf molecule, which in turn forms the shorter of the two H-bonds involved in the dimer motif depicted in Fig. 3 of the main paper. This type of interaction is not found in the structures of **2**-**8**, where the terminal N-atom of the piperazine ring forms H-bonds to water molecules instead.

¶ For the generation of H-stripped Hirshfeld surfaces and the corresponding fingerprint plots, coordinates were obtained from the structures **1**-**6** and **8** listed in Table 1. Only the major disorder component for disordered water O-atoms were considered for the structures of **3**, **5** and **6**. For the structures of **2** and **3**, in which Na is statistically disordered over two sites, we included both orientations of the disordered molecule, with their partial occupancies. This option lets *CrystalExplorer* handle the disorder, and results in a surface based on the smeared electron distribution of an average structure.

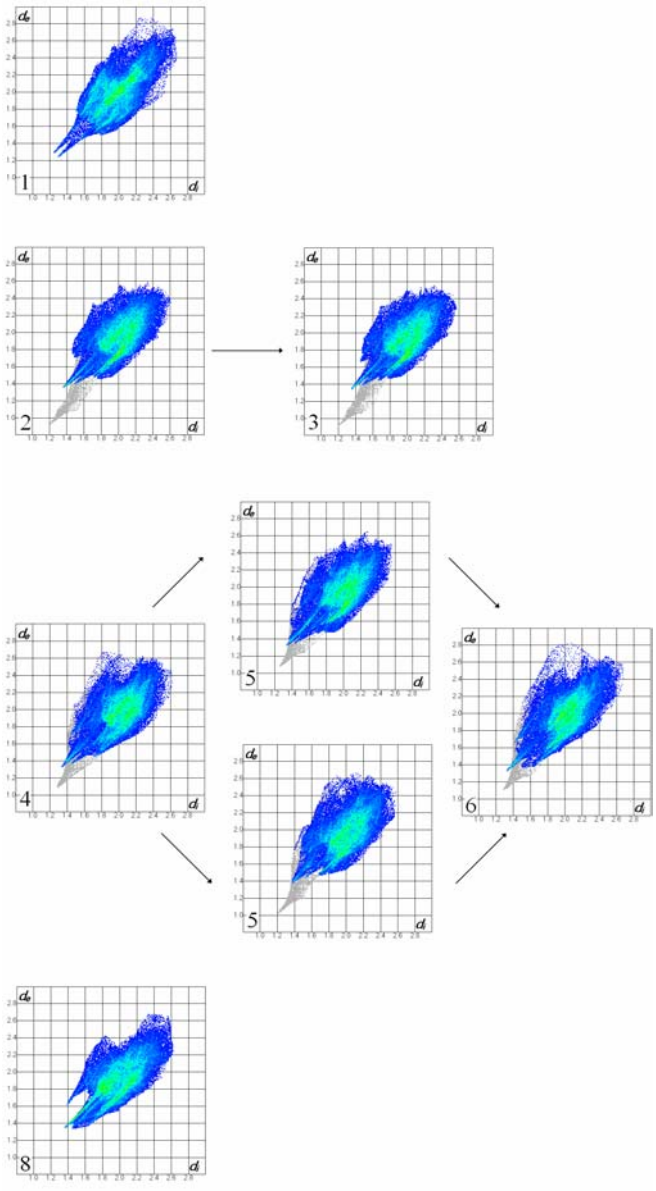

Fig. 4 2-D fingerprint plots derived from H-stripped Hirshfeld surfaces for Cf molecules in the structures **1**-**6** and **8**. The structure of **5** has two Cf molecules in the asymmetric unit. For the structures **2**-**6**, the coloured portions of the plots highlight contacts to all atoms except to sodium. The full fingerprint appears beneath each decomposed plot as a grey shadow.

Comparison of the structures using XPac analysis

The *XPac* method[8] allows the identification of similar packing arrangements that are present in two given molecular crystal structures[9] and produces parameters which characterise their degree of similarity. In the *XPac* approach, each crystal structure is represented by a cluster of molecules, with a central, core molecule and a shell of contacting molecules. The two clusters are then compared by computing the mean differences δ_a and δ_p between the comprehensive (*i.e.* all possible combinations) sets of angles and interplanar angles, respectively, between a chosen group of atoms in the core molecule and the corresponding atoms in one shell molecule (a double subunit) or two shell molecules (a triple subunit). The obtained δ parameters can be considered as reverse indicators of structural similarity.

In the present case, each of the structures **2**-**8** is represented by a cluster composed of a central Cf molecule, surrounded by n = 14 other Cf molecules.$^{\perp}$ Water and Na moieties were not explicitly included in the calculation, but the assembly of Cf molecules will reflect the influence of these components on the packing, to a certain extent. The structure of **1** was not included in the analysis as no similarity, beyond parallel stacking of Cf rings found at high δ values, was identified, *i.e.* the structure of **1** is considerably dissimilar from the other ones investigated here. The initial *XPac* calculations confirmed that the entire Cf assembly is the same in principle for structures **2**-**8**, as intimated earlier from an initial assessment of the main structural features. Much more detailed information, however, can be obtained from *XPac* plots of δ_p against δ_a, as given in Fig. 5. In each plot, there are $n[\ 1 + (n - 1) / 2)] = 105$ data points$^{|}$ (or 210 if 5 with Z' = 2 is involved), and the position of each point characterises the degree of similarity in a particular subunit of the cluster. For a given data point, δ_p is typically more than twice as large as δ_a. All (δ_a, δ_p) points will lie the closer to the origin of the coordinate system the better the two underlying structures match. Thus, a quantitative dissimilarity index X:

$$X = \sum_{i=1}^{M} \left({\delta_{a,i}}^2 + {\delta_{p,i}}^2 \right)^{1/2}$$

can be computed, where X is the mean distance (in °) of all M data points from the origin and $\delta_{a,i}$ and $\delta_{p,i}$ are the coordinates of the i-th data point.

The complete set of X indices is listed in Fig. 6. The *XPac* plot in Fig. 5a is typical for slight structural changes without a phase transition, and it correlates to the anisotropy of the thermal expansion of the hexahydrate between 120 (**8**) and 293 K (**7**). Thus, all data points populate an extremely dense area close to the origin, and X is as low as 1.2°. Significantly less overlap, along with wider δ ranges and a higher X of 2.6° are obtained from the comparison between the hemi Na salt pentahydrate structures **2** and **3**.

The corresponding plot in Fig. 5b illustrates the combined structural effects of changes in pressure and temperature, and the plot characteristics indicate that no phase change has occurred. Furthermore, the relative high δ_p/δ_a ratios suggest that the small structural shifts between **2** and **3** are primarily translational rather than rotational. The vertical and horizontal broken lines indicate the mean δ_a and δ_p values, respectively.

Each of the plots in Fig. 5c-h illustrates the relationship between the hemi Na salt pentahydrate (**2**, **3**) and a structure of the Na salt pentahydrate (**4**-**6**). The relationships between **4**, **5** and **6** are of particular interest. The plots of Fig. 5i and 5j illustrate that the phase transition from **5** to **6** (X = 10.6°) is associated with a more substantial rearrangement of the Cf assembly than that between **4** and **5** (X = 7.9°). In both cases, the data points are scattered along the diagonal, therefore indicating important contributions from both translational and rotational shifts. Although the Cf

arrangements in **4** and **6** are somewhat more similar by comparison (X = 6.2˚), the overall characteristics of the plot (Fig. 5k), in particular the scattered data points, support their interpretation as two distinct phases.

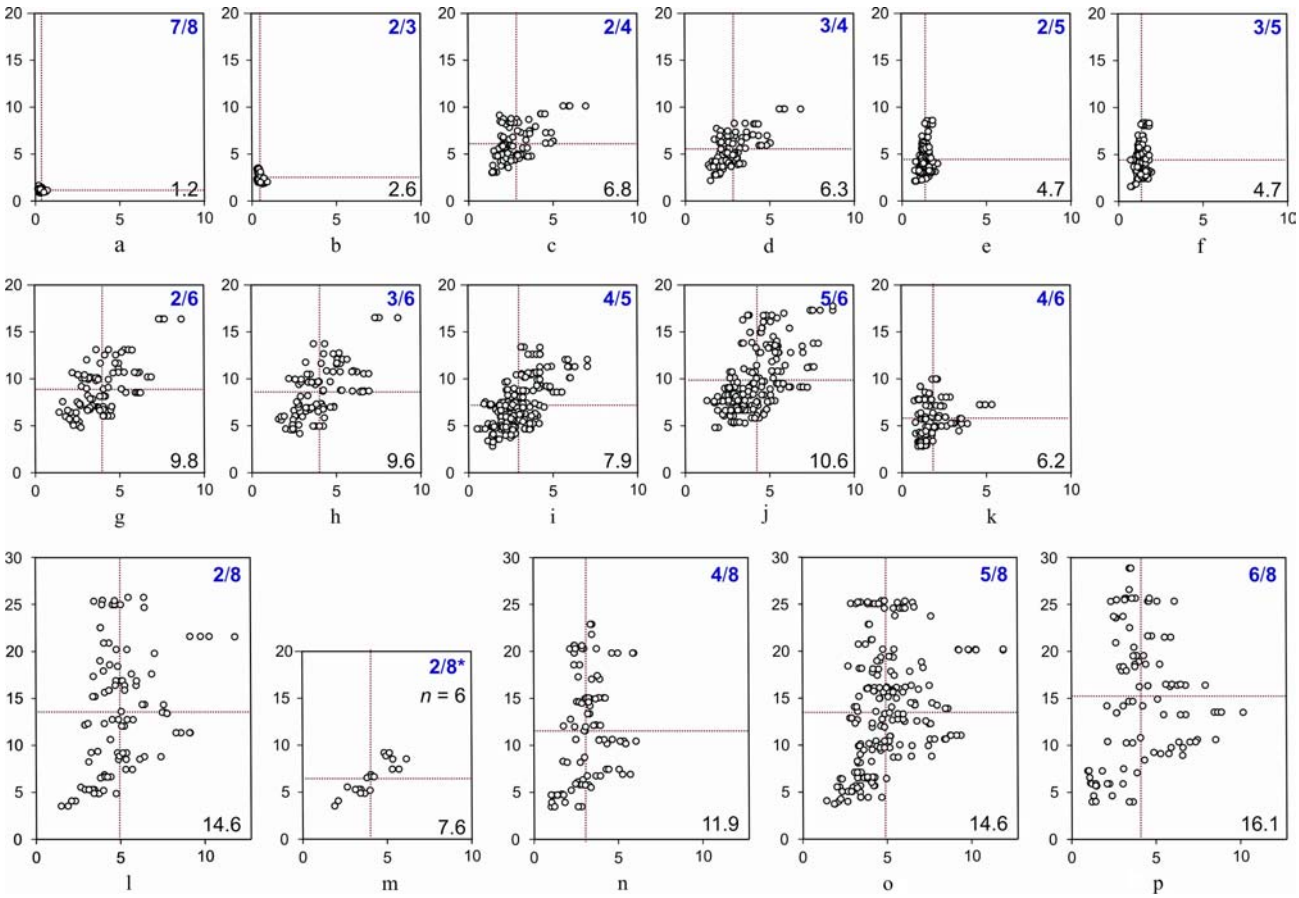

Fig. 5 Selected *XPac* plots δ_p against δ_a (both in ˚), illustrating the degree of similarity exhibited by the Cf assemblies of structures: (a) **7**/**8**, (b) **2**/**3**, (c) **2**/**4**, (d) **3**/**4**, (e) **2**/**5**, (f) **3**/**5**, (g) **2**/**6**, (h) **3**/**6**, (i) **4**/**5**, (j) **5**/**6**, (k) **4**/**6**, (l) **2**/**8** – entire Cf structure with n = 14, (m) **2**/**8** – 2D Cf layer, see Fig. 12, with n = 6 (n) **4**/**8**, (o) **5**/**8**, (p) **6**/**8**. Lower right corner: index X (in ˚), vertical and horizontal broken lines: mean value of δ_a and δ_p, respectively.

All diagrams in Fig. 5 are drawn to the same scale. Figs. 5l, n-p indicate that the level of similarity drops substantially if the hexahydrate (**7**, **8**) is compared to another phase from **2**-**6**. However, a group of data points with low δ_p and low δ_a values can be identified even in these cases. By contrast, disproportionally high δ_p values (relative to δ_a) are calculated for another group of data points. These observations suggest a) that some parts of the compared structures are considerably more similar than others and b) that the most important structural shifts are translational rather than rotational. The plot in Fig. 5m was generated by retaining just 21 of the data points from the preceding Fig. 5l. They characterise a cluster subunit consisting of a central Cf molecule and six out of 14 neighbours. This subunit represents a 2D arrangement of Cf molecules that lies in an *ab*-plane. Both the position of these data points (X = 7.6˚) and their distribution indicate a substantially higher degree of similarity compared to that of the complete Cf structures. This is illustrated in the packing diagrams of Fig. 7, each showing two such 2D Cf fragments. Adjacent Cf layers are stacked in parallel fashion and separated by a layer of either water and Na-cations (**2**-**6**) or just water (**7**, **8**). The geometry of an individual Cf layer is largely retained in **2**-**8**, so that the X index for this structure part is generally low, as evidenced by the last two rows in Fig. 6. However, Fig. 7 shows that there is a considerable difference between **2**-**6** and

the hexahydrate structures (**7**, **8**) with regard to the offset between neighbouring Cf planes. This offset is in turn correlated with the unit cell parameter α (**2**: 85.7° *vs*. **8**: 94.2°). The difference in the offset is likely to occur because there needs to be a suitable coordination environment for Na-cations in **2**-**6** but not in the hexahydrate (**7**, **8**).

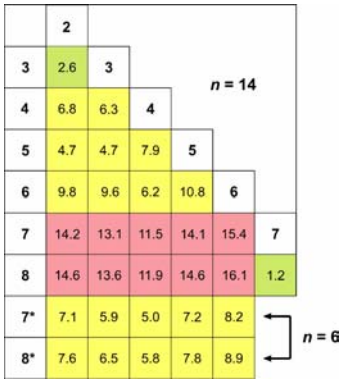

Fig. 11 Dissimilarity index X (in °) for structures **2**-**8** containing Cf. Each box represents the comparison between two crystal structures which can be either identical (green) or different phases with a higher (yellow) or lower(red) degree of similarity. The upper six rows refer to the entire 3D Cf structure (cluster with n = 14), the last two rows (labelled **7***, **8***) just to the Cf layers shown in Fig. 12 (2D, n = 6).

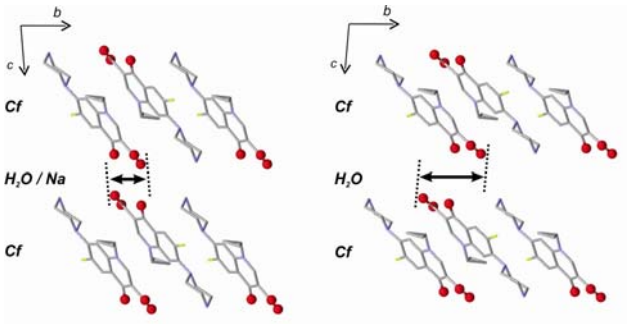

Fig. 7 Packing of Cf molecules in structures **2** (left) and **8** (right), both viewed along the *a*-axis. Each diagram shows two adjacent Cf layers which lie in an *ab*-plane and are separated by either H_2O + Na-cations (**2**) or H_2O (**8**). The arrangement within individual Cf layers is largely unchanged. The different length of the double-headed arrow in each diagram indicates a substantial change in the offset between adjacent Cf layers, which corresponds to the unit cell parameter α. This relationship can be deduced from the *XPac* plots in Figs. 5l -m.

⊥ All calculations were carried out with a representative set of 16 out of 24 non-H atoms of the Cf molecules. No significant change of the results was detected when more atoms were included.
| For a cluster with n shell molecules, one data point is obtained for each of the n double and and (n^2-n)/2 triple subunits.

1 M. Järvinen,. *J. Appl. Crysallogr.*, 1993, **26**, 525-531.
2 A. L. Spek, *PLATON* - A multipurpose Crystallographic Tool, Utrecht University, Utrecht, The Netherlands, 2004.
3 A. Schönleber, P. Pattison and G. Chapuis, *Z. Kristallogr.*, 2003, **218**, 507–513.
4 M. A. Spackman and J. J. McKinnon, *CrystEngComm*, 2002, **4**, 378–392. J. J. McKinnon, M. A. Spackman and A. S. Mitchell, *Acta Crystallogr., Sect. B: Struct. Sci.*, 2004, **60**, 627–668. M. A. Spackman and P. G. Byrom, *Chem. Phys. Lett.*, 1997, **267**, 215–220.
5 See for example: M. A. Spackman and D. Jayatilaka, *CrystEngComm*, 2009, **11**, 19-32; J. J. McKinnon, F. P. A. Fabbiani and M. A. Spackman, *Cryst. Growth Des.*, 2007, **7**, 755-769.
6 A. Parkin, G. Barr, W. Dong, C. J. Gilmore, D. Jayatilaka, J. J. McKinnon, M. A. Spackman and C. C. WIlson, *CrystEngComm*, 2007, **9**, 648-652.
7 D. Grimwood, S. K. Wolff, J. McKinnon, M. Spackman and D. Jayatilaka, Crystal Explorer, University of Western Australia, V. 2.0, build r313.
8 T. Gelbrich and M. B. Hursthouse, *CrystEngComm*, 2005, **7**, 324-336; T. Gelbrich and M. B. Hursthouse, *CrystEngComm*, 2006, **8**, 448-460.
9 See for example: A. J. Florence, C. Bedford, F. P. A. Fabbiani, K. Shankland, T. Gelbrich, M. B. Hursthouse, N. Shankland, A. Johnston and P. Fernandes, *CrystEngComm*, 2008, **10**, 811-813; D. E. Braun, U. J. Griesser, T. Gelbrich, R. K. R. Jetti and V. Kahlenberg, *Cryst. Growth Des*., 2008, **8**, 1977-1989; D. E. Braun, T. Gelbrich, V. Kahlenberg, G. Laus, J. Wieser and U. J. Griesser, *New J. Chem*, 2008, **10**, 1677-1685; T. Gelbrich, D. S. Hughes, M. B. Hursthouse and T. L. Threlfall, *CrystEngComm*, 2008, **10**, 1328-1334.